Preliminary Evaluation of a Low Cost, Austenitic, Ductile Iron

Victoria Rambo
Virginia Tech, Blacksburg, Virginia, USA

Josh Adelmann
SSAB, Mobile, Alabama, USA

Alan Druschitz
Virginia Tech, Blacksburg, Virginia, USA

ABSTRACT

An austenitic ductile iron that does not contain nickel would be a significant achievement since it would reduce cost by eliminating the use of an expensive alloying element. A preliminary evaluation of ductile irons alloyed with 7.5 or 12 wt% manganese (Mn), 1.8-2.0 wt% aluminum (Al), 2.7-2.8 wt% silicon (Si), and no nickel (Ni) has been completed. X-ray diffraction indicated that the microstructures of these ductile irons were predominantly austenite with a small amount (<7%) of martensite/ferrite. The 12 wt% Mn austenitic ductile iron hardened slightly when heat treated and the 7.5 wt% Mn austenitic ductile iron softened significantly when heat treated. The tensile properties for these initial chemistries indicated that additional work is needed to optimize chemistry and heat treatment.

Keywords: austenite, ductile iron, computational materials modeling, stacking fault energy, thermal analysis, manganese, aluminum, X-ray diffraction

INTRODUCTION

Ductile cast iron (also called nodular iron or spheroidal-graphite cast iron) is characterized by graphite in a spheroidal form and free of flake graphite.[1-3] Graphite flakes act like pre-existing cracks since their shape is long with sharp edges. Graphite spheres are compact and have a minimal stress-raising effect. In general, ductile irons have excellent castability. During solidification, the graphite spheroids are the first solid to precipitate (in the liquid) and the formation of low-density graphite during solidification reduces volumetric shrinkage, thus, ductile iron castings generally have small amounts of shrinkage porosity.

Austenitic ductile irons[4] are characterized by spheroidal graphite in a matrix of austenite. Austenite is the non-magnetic, high-temperature form of iron that has a face-centered cubic crystal structure. Austenitic ductile iron castings are often used for their resistance to heat, corrosion, and/or wear. Since austenitic ductile irons do not undergo phase transformations upon heating and cooling and can have high-temperature oxidation resistance, they can be used for applications such as automotive exhaust manifolds. Austenitic ductile irons typically contain 18-37 wt% nickel, which is fairly expensive. The average cost of nickel in 2022 was 11.74 $/lb.[5] The mechanical properties of austenitic ductile irons are typically 210 MPa (30 ksi) yield strength, 380-400 MPa (55-58 ksi) ultimate tensile strength, 6-20% elongation, and 121-202 Brinell hardness.[6]

Austenitic steels can exhibit transformation-induced plasticity (TRIP), or twinning-induced plasticity(TWIP), which can produce a material with the highly desirable combination of high tensile strength and high ductility.[7] The stacking fault energy determines whether TRIP or TWIP will be the dominant mechanism during plastic deformation. TWIP steels have been produced using low-cost manganese, aluminum, and silicon.[8] In 2023, the cost of 99.7% pure electrolytic manganese was 1.10 $/lb to 1.40 $/lb.[9]

The goal of this research was to investigate the potential of using a chemistry range that has shown promise for low carbon content steels,[10-21] nominally 7.5 or 12 w% manganese, 1.5-2 wt% aluminum, and 2-3 wt% silicon, for ductile iron castings. The chemistry (Mn, Al, Si, C in solution) was chosen to produce a stacking fault energy (SFE) greater than about 19 mJ/m,[2] which should produce a cast iron that exhibits TWIP.[22] Anticipated problems with this chemistry are: 1) manganese is known to promote carbides when greater than about 0.70 wt% and 2) aluminum is known to promote vermicular graphite when greater than about 0.06 wt%.[23]

EXPERIMENTAL METHODS

A commercial computational materials modeling software package[24] was used to characterize potential compositions for investigation. The predicted phase diagrams were

examined and specific target chemistry ranges were chosen. The liquidus and solidus temperatures for the target chemistries were determined to aid in developing appropriate pouring temperatures. The software was also used to predict the appropriate temperature for heat treatment.

Stacking fault energy (SFE) for the target chemistries was predicted since TWIP is only expected to occur if the SFE is greater than about 19 mJ/m.[2] The equations used to predict SFE were:

$$SFE\ (mJ/m^2) = (2000 * \text{molar surface density} * \Delta G_{total}) + (2 * \sigma^{\gamma-\varepsilon}) \quad \text{Eqn. 1}^{8}$$

$$\Delta G_{total}\ (J/mol) = \Delta G_{chem} + \Delta G_{mag} + \Delta G_{ex} \quad \text{Eqn. 2}^{8}$$

$$\Delta G_{chem}\ (J/mol) = -422.6X_{Fe} + 3460X_{Mn} + 4941.34X_{Al} - 2960X_{Si} - 24595.1X_{C} - 7973.89\ X_{Fe}X_{Mn} + 3323X_{Fe}X_{Al} + 1780X_{Fe}X_{Si} + 42500X_{Fe}X_{C} + 26910X_{Mn}X_{C} \quad \text{Eqn. 3}^{8}$$

$$\Delta G_{ex}\ (J/mol) = 170.06 * \exp(-d/18.55) \quad \text{Eqn. 4}^{8}$$

Where:
molar surface density = 2.929×10^{-5} m^3/mol,
$\sigma^{\gamma-\varepsilon} = 10$,
$\Delta G_{mag} = 0.004$ J/mol,
X_{Fe} = mole fraction of Fe,
X_{Mn} = mole fraction of Mn,
X_{Al} = mole fraction of Al,
X_{Si} = mole fraction of Si,
X_{C} = mole fraction of C, and
d = grain size in microns.

Manganese, carbon, and silicon decrease the martensite start temperature while aluminum increases the martensite start temperature. The equation used to determine the martensite start temperature, M_S, was Eqn. 5.[25]

$$M_S\ (^oC) = 539 - 426 \times wt\%\ C - 30.4 \times wt\%\ Mn - 7.5 \times wt\%\ Si + 30 \times wt\%\ Al \quad \text{Eqn. 5}^{25}$$

Two 47 kg heats were prepared in a 150 kg capacity induction furnace lined with a high alumina crucible. The charge materials for the base iron were pig iron, ductile iron scrap, plain carbon steel, carbon raiser, electrolytic manganese, commercially pure aluminum, and scrap Fe30Mn4Al1Si0.9C0.5Mo. Ultra-high purity argon (spectrometer grade) at a flow rate of 0.28 m^3/hour was used as a cover gas to reduce the amount of oxidation and nitrogen pick-up during melting. The sandwich treatment method was used to produce ductile iron. Treatment was performed in an 80 kg, pre-heated crucible that had a pocket to improve recovery. The treatment charge materials were foundry grade 75%FeSi, Ba-containing 50%FeSi, and 4.5%MgFeSi. A small amount (0.15 wt%) Bi-containing 75%FeSi was added to each mold. Treatment temperature was between 1515C (2760F) and 1550C (2820F).

Rectangular plates, 12.7 mm x 150 mm x 230 mm (0.5” x 6” x 9”) and Y-blocks for castings of thickness 13 mm (0.5”) to 38 mm (1.5”) per ASTM A439, were cast in silica sand molds bonded with phenolic urethane resin. Chemistry samples and thermal analysis samples were taken during pouring. The liquidus and solidus of the 7.5 wt% Mn austenitic ductile iron were measured using a type K thermocouple. The thermocouple tip was located in the middle of a shell sand mold that produced a 35 mm x 35 mm x 40 mm tall rectangular prism. The thermocouple was connected to an analog-to-digital converter connected to a laptop computer. Measurements were taken every one second and the data was analyzed using Excel.

Inductively coupled plasma-mass spectrometry (ICP-MS) was used to determine the manganese, aluminum, silicon, magnesium, and molybdenum contents, and combustion analysis was used to determine the carbon and sulfur contents.

Brinell hardness was determined following ASTM E10-18.[26] Samples were ground to an 80 grit surface finish and hardness was determined using a 10 mm diameter tungsten carbide ball, 3000 kg load, and a load time of 12 seconds. The diameter of the impression was measured in at least two directions and the impression diameters converted to HBW.

Microstructure was determined using standard metallographic techniques. Samples were ground on successively finer grit SiC paper (240, 320, 400, 600, 1200) followed by polishing with 1-micron diamond paste. Metallography samples were examined in the as-polished and etched condition. A solution of 3% Nital was used to etch the samples.

Phases present were determined using X-ray diffraction (XRD) with Cu-K_α radiation. Rietveld refinement, phase identification, phase quantification, and the export of graphical results were performed using an open-source software package.[27]

To determine if any phase transformations occurred during heating and cooling, a 2 mm (5/64”) diameter hole was drilled into samples, and 1.5 mm (1/16”) diameter, type K thermocouples were inserted into the holes. Solid carbide and straight flute drills were used to make the holes. Thermocouples were connected to an analog-to-digital converter connected to a laptop. Measurements were taken every one second and the data was analyzed using Excel.

Tensile properties were determined per ASTM E8[28] by an outside lab. Blanks with approximate dimensions of 19

mm x 19 mm x 165 mm (0.75” x 0.75” x 6.5”) were cut from the Y-blocks using a carbide grit band saw blade. The blanks from the 12 wt% Mn austenitic ductile iron were heat treated at 831C (1528F) for two hours followed by air cooling to room temperature and the blanks from the 7.5 wt% Mn austenitic ductile iron were heat treated at 877C (1611F) for two hours followed by air cooling to room temperature. Round tensile bars of 12.8 mm (0.505”) diameter and 50.8 mm (2.0”) gage length were machined from the heat-treated blanks. Room temperature 0.2% offset yield strength, ultimate tensile strength, elongation at failure, reduction in area, and elastic modulus were determined.

RESULTS AND DISCUSSION

The target chemistry for the first heat was 12Mn2Al2.5Si3.5C. The actual chemistry was reasonably close; the aluminum content was slightly low, the silicon content slightly high, and the Mg content slightly low, Table 1.

Table 1. Chemical Composition (wt%) for 12 wt% Mn Austenitic Ductile Iron

	Mn	Al	Si	C	Mg	Mo	S	Fe
Target	11-13	1.6-2.2	2.0-3.0	3.2-3.6	0.035-0.050	<0.20	<0.015	balance
Actual	12.04	1.79	2.72	3.58	0.032	0.18	0.0065	balance

The as-cast material was only slightly attracted to a magnet, which indicated that the microstructure was most likely predominantly austenite. Samples of the 12 wt% austenitic ductile iron were heated to 831C (1528F) and held for two or 14 hours to put approximately 1.0 wt% carbon into the solution, followed by air cooling or water quenching. When measuring Brinell hardness, some of the samples cracked adjacent to the hardness impressions, which indicated that these samples had low ductility. The hardness of the 12 wt% austenitic ductile iron was significantly higher compared to the ASTM A439 specification. The hardness of the as-cast and heat-treated samples are listed in Table 2.

Table 2. Brinell Hardness of As-cast and Heat Treated 12 wt% Mn Austenitic Ductile Iron

Condition	Brinell Hardness
As-Cast	298 +/- 7
Heat treated 831C (1528F)/2 hrs	296 +/- 7
Heat treated 831C (1528F)/24 hrs	306 +/- 4
Heat treated 831C (1528F)/96 hrs	309 +/- 3

The microstructure for the 12 wt% Mn austenitic ductile iron appeared to have a two-phase matrix microstructure plus a mixture of vermicular and spheroidal graphite. The nodularity was estimated to be 70% using ASTM A247.[29] The interdendritic phase was still present after heat treatment at 831C (1528F) for 96 hours. The as-polished and etched microstructures of the 12 wt% Mn austenitic ductile iron are shown in Figures 1-6.

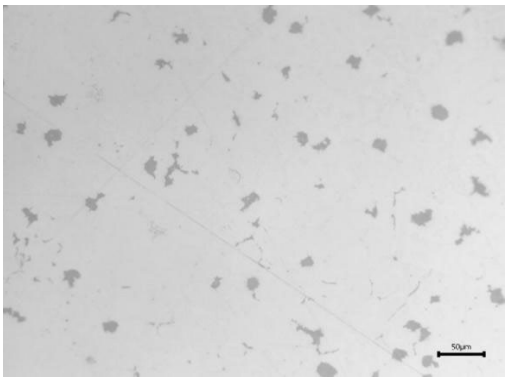

Figure 1. Microstructure of the 12 wt% Mn austenitic ductile iron as-cast (as-polished).

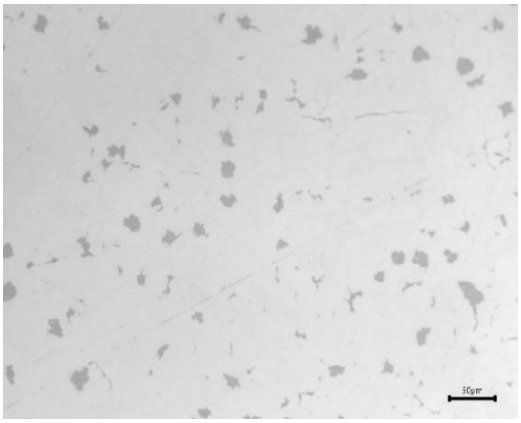

Figure 2. Microstructure of the 12 wt% Mn austenitic ductile iron heat treated at 831C (1528F) for two hours (as-polished).

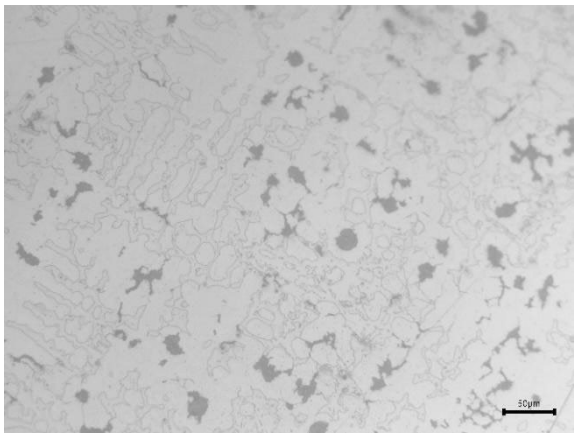

Figure 3. Microstructure of the 12 wt% Mn austenitic ductile iron as-cast (etched in 3% Nital).

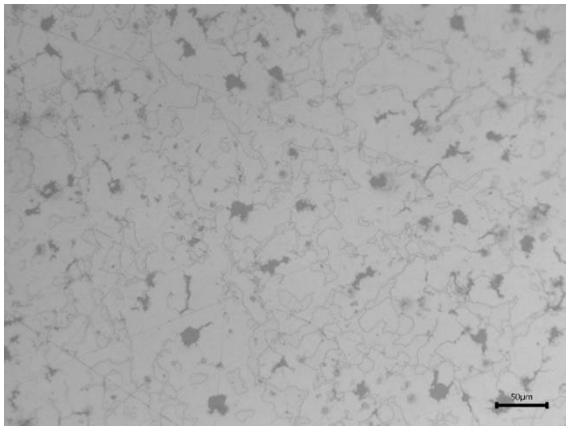

Figure 4. Microstructure of the 12 wt% Mn austenitic ductile iron heat treated at 831C (1528F) for two hours (etched in 3% Nital).

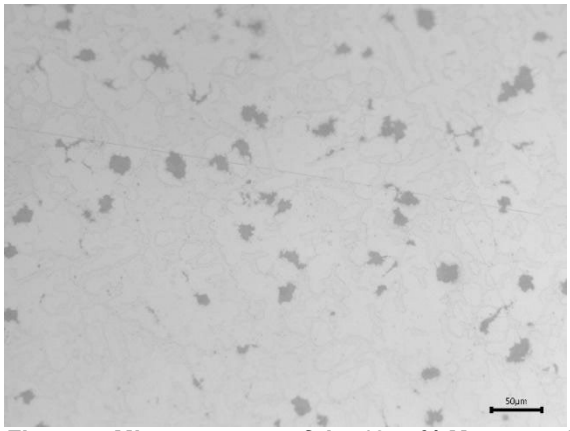

Figure 5. Microstructure of the 12 wt% Mn austenitic ductile iron heat treated at 831C (1528F) for 24 hours (etched in 3% Nital).

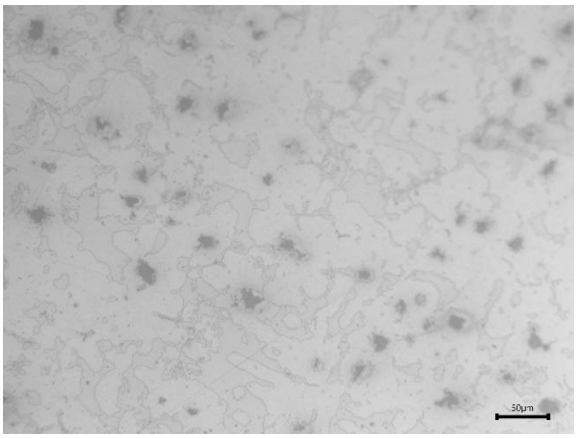

Figure 6. Microstructure of the 12 wt% Mn austenitic ductile iron heat treated at 831ºC (1528F) for 96 hours (etched in 3% Nital).

X-ray diffraction determined that the phase present in all as-cast and heat-treated samples was predominantly austenite, as expected. Quantitative analysis using the open source software indicated that the as-cast sample was 88% austenite, 6% martensite/ferrite, and 5.5% graphite and the sample heat-treated at 831C (1528F) for two hours, followed by air cooling was 90% austenite, 6% martensite/ferrite, and 3.5% graphite. The calculated Ms temperature for the 12 wt% Mn austenitic ductile iron was -220C (-364F) for 1 wt% carbon in solution so no martensite would be expected in the microstructure unless this martensite formed by transformation-induced plasticity (TRIP) during sample preparation. However, the stacking fault energy for the 12 wt% Mn austenitic ductile iron was 24 mJ/m^2, which indicated that TRIP should not occur. Since the heat-treated sample was not exceptionally hard, which would indicate the presence of martensite, and was slightly attracted to a magnet, some ferrite, rather than martensite, may have been present. The X-ray diffraction data for as-cast and heat treated at 831C (1528F) for two hours, followed by air cooling is shown in Figures 7 and 8.

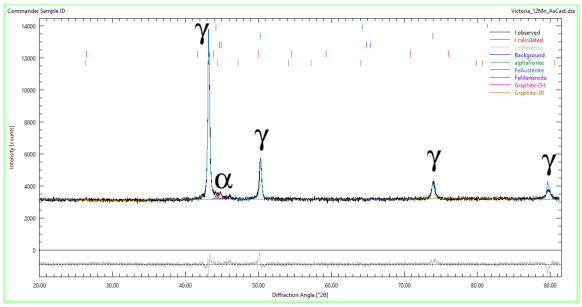

Figure 7. X-ray diffraction data for the 12 wt% Mn austenitic ductile iron as-cast shows the microstructure to be predominantly austenite.

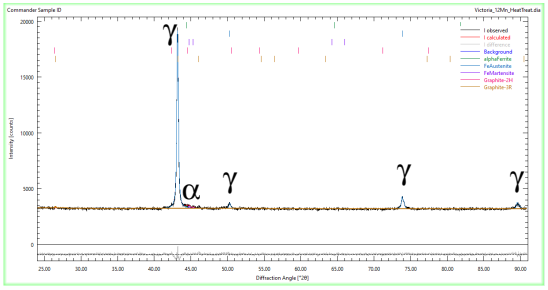

Figure 8. X-ray diffraction data for the 12 wt% Mn austenitic ductile iron heat treated at 831C (1528F) for two hours, followed by air cooling showing the microstructure to be predominantly austenite.

No phase transformations were observed for the 12 wt% Mn austenitic ductile iron when the thermocouple sample was heated to 834C (1533F), which indicated that the austenite present was stable down to room temperature and little or no ferrite or martensite was present. The thermal analysis data for the 12 wt% Mn austenitic ductile iron upon heating in the solid state is shown in Figures 9 & 10.

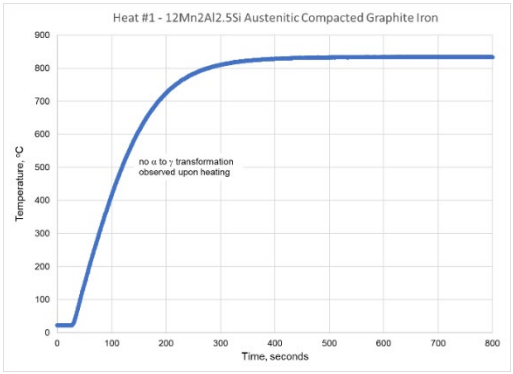

Figure 9. Temperature vs time data during heating in the solid state for the 12 wt% Mn austenitic ductile iron.

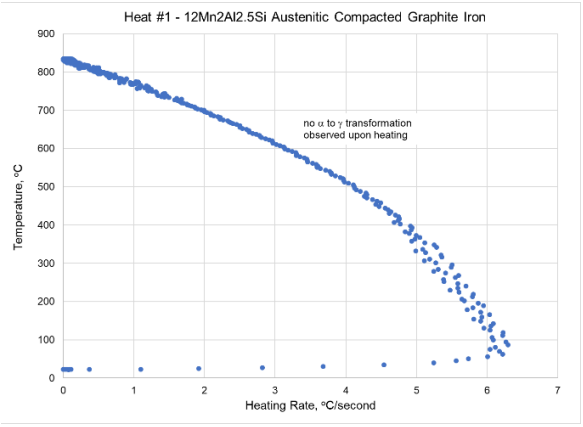

Figure 10. Temperature vs. heating rate data in the solid state for the 12 wt% Mn austenitic ductile iron.

The tensile properties (average of three tests) for the 12 wt% Mn austenitic ductile iron heat treated at 831°C for two hours followed by air cooling to room temperature were 276 +/- 31 MPa (40.1 +/- 4.4 ksi) ultimate tensile strength, 1.7 +/- 0.2% elongation at failure, 0.6 +/- 0.3% reduction in area, and 149 +/- 8 GPa (21.7 +/- 1.2 mpsi) elastic modulus. A 0.2% offset yield strength could not be determined due to the low elongation at failure.

The target chemistry for the second heat was 8Mn2Al2.6Si3.5C. The actual chemistry was reasonably close; the Mg content was higher than expected and may indicate that the chemistry sample had Mg-containing slag/dross inclusions, Table 3.

Table 3. Chemical Composition (wt%) for 7.5 wt% Mn Austenitic Ductile Iron

	Mn	Al	Si	C	Mg	Mo	S	Fe
Target	7-9	1.6-2.2	2.0-3.0	3.2-3.6	0.035-0.050	<0.20	<0.015	balance
Actual	7.55	2.03	2.78	3.22	0.084*	0.10	0.011	balance

* chemistry sample may have had Mg-containing slag/dross inclusions

The liquidus and solidus of the 7.5 wt% Mn austenitic ductile iron were measured by thermal analysis. The measured liquidus was 1182C (2160F) and the measured solidus was 1118C (2044F). The liquidus and solidus for this chemistry predicted by the software package were 1250C (2282F) and 1197C (2187F), respectively.

The predicted values were significantly higher (68°C/122.4°F higher for liquidus and 79°C/142.2°F higher for solidus) than the measured values. The thermal analysis for the 7.5 wt% Mn austenitic ductile iron during solidification is shown in Figures 11 & 12.

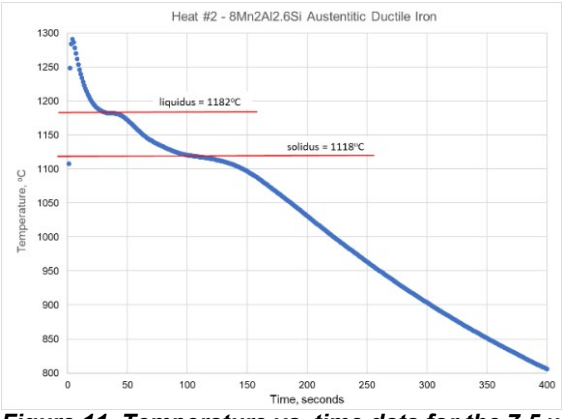

Figure 11. Temperature vs. time data for the 7.5 wt% Mn austenitic ductile iron during solidification.

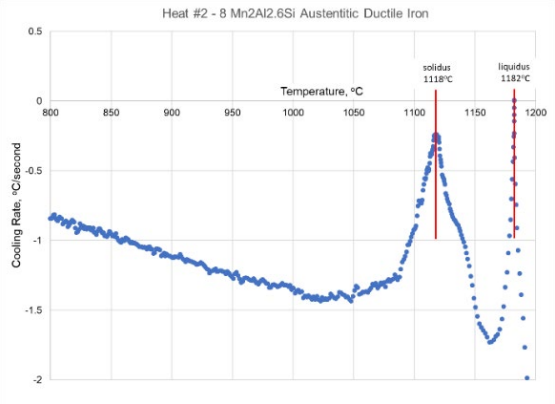

Figure 12. Cooling rate vs. temperature data for the 7.5 wt% Mn austenitic ductile iron during solidification.

The as-cast material was only slightly attracted to a magnet, which indicated that the microstructure was most likely predominantly austenite. Samples of the 7.5 wt% Mn austenitic ductile iron were heated to 877C (1611F) and held for various amounts of time to put approximately 1.0 wt% carbon into the solution, followed by air cooling. Heating to 877C (1611F) for two hours followed by air cooling reduced the hardness from 260 BHN to 238 BHN and the hardness was only 216 BHN after heat treatment at 877C (1611F) for 96 hours, which was just a little bit higher than the upper limit in the ASTM A439 specification. The hardness of the as-cast and heat-treated samples are listed in Table 4.

Table 4. Brinell Hardness of As-cast and Heat Treated 7.5 wt% Mn Sample

Condition	Brinell Hardness
As-Cast	260 +/- 6
Heat Treated 877C (1611F)/2 hrs	238 +/- 7
Heat Treated 877C (1611F)/24 hrs	230 +/- 2
Heat Treated 877C (1611F)/96 hrs	216 +/- 6

The microstructure for the 7.5 wt% Mn austenitic ductile iron appeared to have a two-phase matrix microstructure plus predominantly spheroidal graphite. The nodularity was estimated to be 90% using ASTM A247. Unlike the 12 wt% Mn austenitic ductile iron, the interdendritic network appeared to be predominantly gone after heat treatment at 877C (1611F) for 96 hours, which may be responsible for the reduction in hardness. The microstructures of the 7.5 wt% Mn austenitic ductile iron in the as-polished and etched conditions are shown in Figures 13-18.

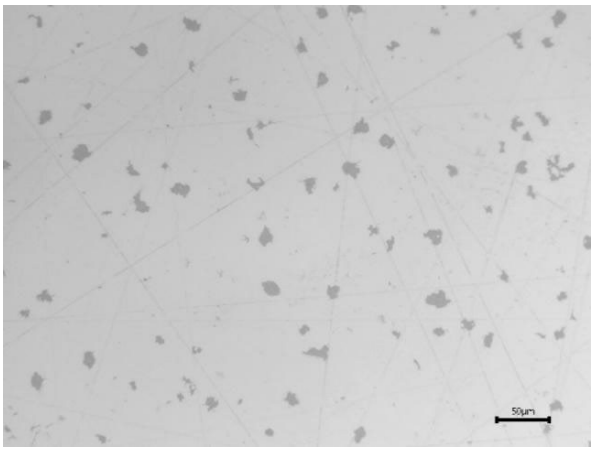

Figure 13. Microstructure of the 7.5 wt% Mn austenitic ductile iron as-cast (as-polished).

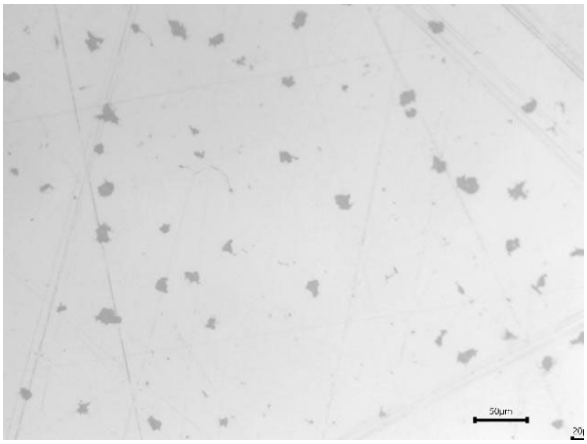

Figure 14. Microstructure of the 7.5 wt% Mn austenitic ductile iron heat treated at 877C (1611F) for two hours (as-polished).

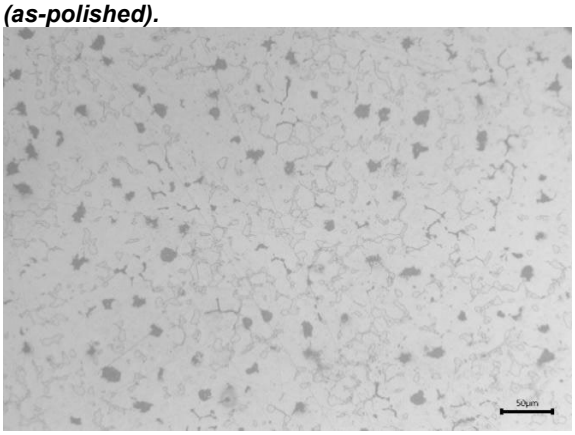

Figure 15. Microstructure of the 7.5 wt% Mn austenitic ductile iron as-cast (etched in 3% Nital).

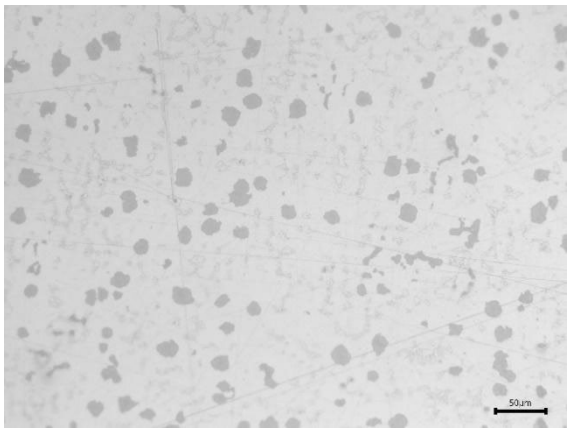

Figure 16. Microstructure of the 7.5 wt% Mn austenitic ductile iron heat treated at 877C (1611F) for two hours (etched in 3% Nital).

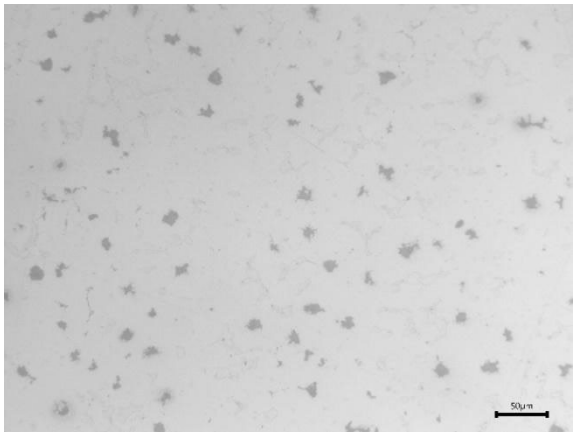

Figure 17. Microstructure of the 7.5 wt% Mn austenitic ductile iron heat treated at 877C (1611F) for 24 hours (etched in 3% Nital).

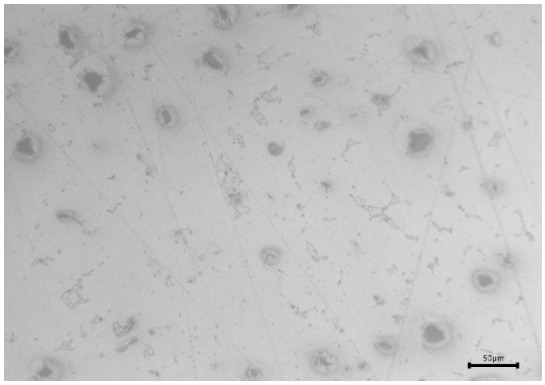

Figure 18. Microstructure of the 7.5 wt% Mn austenitic ductile iron heat treated at 877C (1611F) for 96 hours (etched in 3% Nital).

X-ray diffraction determined that the phase present in all as-cast and heat-treated samples was predominantly austenite, as expected. Quantitative analysis using open source software indicated that the as-cast sample was 88% austenite, 7% martensite/ferrite, and 4% graphite, and the sample heat-treated at 877C (1611F) for two hours, followed by air cooling was 83% austenite, 4% martensite/ferrite, and 13% graphite. The calculated Ms temperature for the 7.5 wt% Mn austenitic ductile iron was -73°C (-99.4°F) for 1 wt% carbon in solution so no martensite would be expected in microstructure unless this martensite formed by transformation-induced plasticity (TRIP) during sample preparation. However, the stacking fault energy for the 7.5 wt% Mn austenitic ductile iron was 30 mJ/m^2, which indicated that TRIP should not occur. Since the as-cast sample was slightly harder than the heat-treated sample (260 BHW vs 238 HBW), there may have been a small amount of martensite, ferrite, or Fe_3C present in the as-cast samples, which would explain why these samples were slightly attracted to a magnet. The X-ray diffraction data for as-cast and heat treated at 877C (1611F) for two hours, followed by air cooling is shown in Figures 19 & 20.

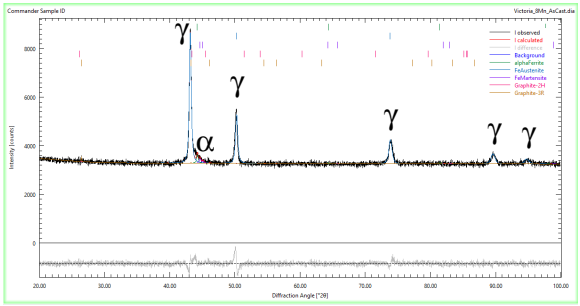

Figure 19. X-ray diffraction data for the 7.5 wt% Mn austenitic ductile iron as-cast shows the microstructure to be predominantly austenite.

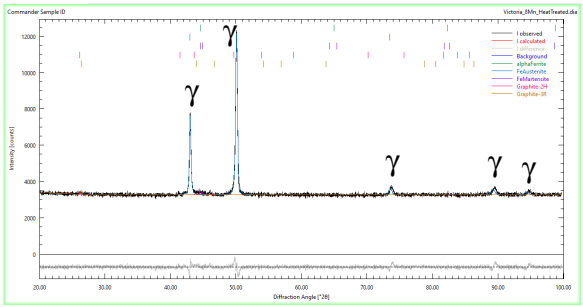

Figure 20. X-ray diffraction data for the 7.5 wt% Mn austenitic ductile iron heat treated at 877C (1611F) for two hours, followed by air cooling showing the microstructure to be predominantly austenite.

No phase transformations were observed for the 7.5 wt% Mn austenitic ductile iron when a thermocouple sample was heated to 878C (1613F), which indicated that the austenite present was stable down to room temperature and little or no ferrite or martensite was present. The thermal analysis data for Heat #2 during heating in the solid state is shown in Figures 21 & 22.

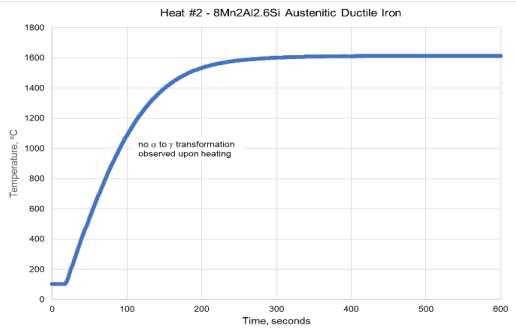

Figure 21. Temperature vs time data during heating in the solid state for the 7.5 wt% Mn austenitic ductile iron.

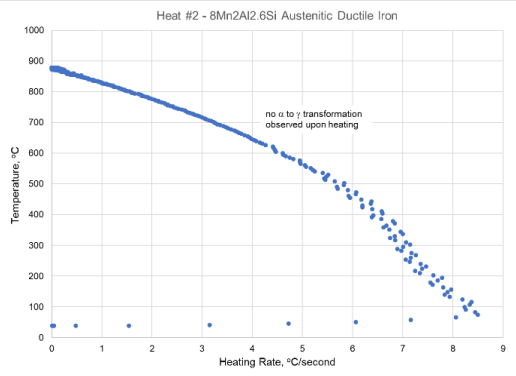

Figure 22. Temperature vs heating rate data in the solid state for the 7.5 wt% Mn austenitic ductile iron.

The tensile properties (average of three tests) for Heat 2 heat treated at 877C (1611F) for two hours followed by air cooling to room temperature were 421 +/- 8 MPa (61.1 +/- 1.2 ksi) 0.2% offset yield strength, 452 +/- 51 MPa (65.6 +/- 7.4 ksi) ultimate tensile strength, 1.7 +/- 0.6% elongation at failure, 0.9 +/- 0.6% reduction in area, and 149 +/- 3 GPa (21.7 +/- 0.5 mpsi) elastic modulus.

CONCLUSIONS

1. Austenitic ductile iron can be produced using manganese and aluminum rather than nickel.
2. The nodularity of the austenitic ductile irons produced using manganese and aluminum was 70% for the 12 wt% Mn and 90% for the 7.5 wt% Mn.
3. The 7.5 wt% Mn austenitic ductile iron was softer than the 12 wt% Mn austenitic ductile iron in the as-cast condition.
4. After heat treating to put approximately 1 wt% carbon into solution the hardness was reduced compared to as-cast for the 7.5 wt% Mn austenitic ductile iron and increased for the 12 wt% Mn austenitic ductile iron.
5. The mechanical properties of a 7.5 wt% Mn austenitic ductile iron were better (higher strength, higher elongation at failure) than a 12 wt% Mn austenitic ductile iron.
6. Compared to the ASTM A439 specification, the yield and ultimate tensile strength of the Mn austenitic ductile irons were much higher than the specification but the elongation at failure was much lower.

FUTURE WORK

Electron microprobe analysis will be performed to characterize the segregation of alloying elements in the as-cast condition. Scanning electron microscopy, energy dispersive spectroscopy, and electron backscatter diffraction (EBSD) will be performed to more thoroughly characterize the microstructure in the as-cast and heat-treated condition. EBSD will clarify if martensite/ferrite is present.

Additional chemistries (lower Mn content) will be investigated to more thoroughly determine the effect of Mn on microstructure and mechanical properties.

ACKNOWLEDGEMENTS

The authors would like to acknowledge Sophie Calandra, who helped during melting and pouring, and Drew Kalil, who performed the X-ray diffraction analysis. NSL Analytical, Cleveland, Ohio ran the ICP-MS for determining chemistry and Westmoreland Mechanical Testing & Research, Youngstown, PA performed the tensile testing.

REFERENCES

1. "ASM Specialty Handbook, Cast Iron," edited by J.R. Davis, ASM International, Materials Park, OH, pp. 54-79 (1996).
2. "The Sorelmetal Book of Ductile Iron," Rio Tinto Iron & Titanium, Inc., Montreal, Quebec, p. 7 (2004).
3. Schleg, Fred, "Technology of Metalcasting," American Foundry Society, Schaumburg, IL, pp. 88-89 (2003).
4. "Ductile Iron Handbook," M. Burditt (editor), American Foundrymen's Society, Inc., Des Plaines, IL, pp. 52-65 (1992).
5. Statistica (Link last accessed 02-08-24.) https://www.statista.com/statistics/236578/iron-ore-prices-since-2003/
6. "Standard Specification for Austenitic Ductile Iron Castings," A439/A439M, ASTM International, 100 Barr Harbor Drive, West Conshohocken, PA (2022). DOI: 10.1520/A0439_A0439M-18R22
7. Hu, B., Luo, H., Yang, F., and Dong, H., "Recent progress in medium-Mn steels made with new designing strategies, a review," *Journal of Materials Science & Technology*, 33 (2017). 1457-1464. DOI: 10.1016/j.jmst.2017.06.017

8. Saeed-Akbari, A., Imlau, J., Prahl, U., and Bleck, W., "Derivation and Variation in Composition-Dependent Stacking Fault Energy Maps Based on Subregular Solution Model in High-Manganese Steels," *Met. Trans. A*, Vol. 40A, 3072-3090 (Dec. 2009). DOI: 10.1007.s11661-009-0050-8
9. Argus Media (Link last accessed 04-08-24.) https://www.argusmedia.com/metals-platform/price/assessment/manganese-electrolytic-metal-min-99-7--fob-us-warehouse-prices-PA00157280000
10. Lee, S. and De Cooman, B.C., "Annealing Temperature Dependence of the Tensile Behavior of 10 pct Mn Multi-phase TWIP-TRIP Steel," *Metallurgical and Materials Transactions A,* Vol 45A, 6039-6052 (Dec 2014). DOI: 10.1007/s11661-014-2540-6
11. Aydin, H., Jung, In-Ho, Essadiqi, E., and Yue, S., "Twinning and Tripping in 10% Mn steels," *Materials Science & Engineering A*, 591, 90-96 (2014). DOI: 10.1016/j.msae.2013.10.088
12. Lee. S., Lee, K., and De Cooman, B.C., "Observation of the TWIP + TRIP Plasticity-Enhancement Mechanism in Al-Added 6 Wt Pct Medium Mn Steel," *Metallurgical and Materials Transactions A,* Vol 46A, 2356-2363 (June 2015). DOI: 10.1007/s11661-015-2854-z
13. Lee, C-Y., J, J., Han, J., Lee, S-J., Lee, S., and Lee, Y-K., "Coupled strengthening in a medium manganese lightweight steel with an inhomogenously grain structure of austenite," *Acta Materialia* 84, 1-8 (2015). DOI: 10.1016/j.actamat.2014.10.032
14. Lee, S. and De Cooman, B.C., "Tensile Behavior of Intercritically Annealed Ultra-Fine Grained 8% Mn Multi-Phase Steel," *Steel Research Int.* 86, No. 10, pp. 1170-1178 (2015). DOI: 10.1002/srin.201500038
15. Lee, S., Woo, W., and De Cooman, B.C., "Analysis of the Tensile Behavior of 12 pct Mn Multi-phase (α + γ) TWIP + TRIP Steel by Neutron Diffraction," *Metallurgical and Materials Transactions A*, Vol 47A, 2016-2125 (May 2016). DOI: 10.1007/s11661-016-3407-9
16. Yan, S., Liang, T., Wang, Z., Yan, B., Li, T., and Liu, X., "Novel 1.4 GPa strength medium-Mn steel with uncompromised high ductility," *Materials Science & Engineering A*, 773, 138732 (2020). DOI: 10.1016/j.msea.2019.138732
17. Kwok, T.W.J., Rahman, K.M., Xu, X., Bantounas, I., Kelleher, J.F., Dasari, S., and Alam, T., "Design of a high strength, high ductility 12 wt% Mn medium manganese steel with hierarchical deformation behavior," *Materials Science & Engineering A*, 782, 139258 (2020). DOI: 10.1016/j.msea.2020.139258
18. Kwok, T.W.J., Gong, P., Xu, X., Nutter, J., Rainforth, W.M., and Dye, D., "Microstructure evolution and tensile behaviour of a cold rolled 8 wt% Mn medium manganese steel," *Metall. Mater. Trans. A*, (July 2021).
19. Shao, C., Hui, W., Zhang, Y., Zhao, X., and Weng, Y., "Microstructure and mechanical properties of hot-rolled medium-Mn steel containing 3% aluminum," *Materials Science & Engineering A*, 682, 44-53(2017). DOI: 10.1016/j.msea.2016.11.036
20. Sun, B., Fazeli, F., Scott, C., Brodusch, N., and Gauvin, R., "The influence of silicon additions on the deformation behavior of austenite-ferrite duplex medium manganese steels," *Acta Materialia*, 148, 249-262 (2018). DOI: 10.1016/j.actamat.2018.02.005
21. A. Druschitz, A. Carnahan, S. Stivala, A. Kalil, "Medium-Manganese FeMnAiAlC Advanced High-Strength Steels," *Proceedings of the International Symposium on New Developments in Advanced High-Strength Sheet Steels*, Vail, CO (June 19-22, 2023) Association of Iron and Steel Technology, 186 Thorn Hill Road, Warrendale, PA, pp. 194-202 (2023).
22. De Cooman, B.C., Estrin, Y., and Kim, S.K., "Twinning-induced plasticity (TWIP) steels," *Acta Materialia,* 142, 283-362 (2018). http://dx.doi.org/10.1016/j.actamat.2017.06.046
23. "ASM Specialty Handbook, Cast Irons," edited by J.R. Davies, ASM International, Materials Park, OH, p. 60 (1996).
24. Thermo-Calc Software, (Link last accessed 04-08-24.) https://thermocalc.com/
25. Mahieu, J., Maki, J., De Cooman, B.C., and Claessens, S., "Phase Transformation and Mechanical Properties of Si-Free CMnAl Transformation-Induced Plasticity-Aided Steel," *Metallurgical and Materials Transactions A*, Vol 33A, 2573-2580 (Aug 2022).
26. ASTM E10-18, "Standard Test Methods for Brinell Hardness of Metallic Materials," ASTM International, 100 Barr Harbor Drive, West Conshohocken, PA (2018). DOI: 10.1520/E0010-18
27. Profex (Link last accessed 04-08-24.) https://www.profex-xrd.org/
28. ASTM E8/E8M - 21, "Standard Test Methods for Tension Testing of Metallic Materials," ASTM International, 100 Barr Harbor Drive, West Conshohocken, PA 19428-2959 (2021) 4. DOI: 10.1520/E0008_E0008M-16AE01
29. ASTM A247-19, "Standard Test Methods for Evaluating the Microstructure of Graphite in Iron Castings," ASTM International, 100 Barr Harbor Drive, West Conshohocken, PA (2019) DOI: 10.1520/A0247-19